AJAB

Asian J Agric & Biol. xxxx(x).
DOI: 10.35495/ajab.2023.182

Original Article

A new nanofibre derived from *Trichoderma hamatum* K01 to control durian rot caused by *Phytophthora palmivora*

Pheaktra Phal[1*], Kasem Soytong[1,2], Supattra Poeaim[3]

[1]Department of Plant Production Technology, School of Agricultural Technology, King Mongkut's Institute of Technology Ladkrabang (KMITL), Ladkrabang, Bangkok 10520, Thailand

[2]Research Institute of Modern Organic Agriculture, King Mongkut's Institute of Technology Ladkrabang (KMITL), Ladkrabang, Bangkok 10520, Thailand

[3]Department of Biology, School of Science, King Mongkut's Institute of Technology Ladkrabang (KMITL), Ladkrabang, Bangkok 10520, Thailand

Received:
September 07, 2023

Accepted:
October 28, 2023

Published Online:
November 27, 2023

**Corresponding author email:*
62604009@kmitl.ac.th

Abstract

Phytophthora rot of durian var Monthong caused by *Phytophthora palmivora* has been proven to be a serious threat to durian plantations in Thailand. The research was targeted to isolate the causal pathogen and prove its pathogenicity by Koch's postulate. Morphology and molecular phylogeny have confirmed the identification of pathogenic and antagonistic fungi. Evaluation of antagonistic fungus against plant pathogen in vitro and greenhouse conditions, morphology and molecular phylogenetic identification confirmed antagonistic species *Trichoderma hamatum* K01 and pathogenic isolate *P. palmivora* PYSC01. The crude metabolite of *T. hamatum* K01, namely TK01-MeOH gave the most substantial inhibitory effect to inhibit colony growth and sporangia formation at ED_{50} (50% effective dose) values of 288 and 118 µg/mL, respectively. Moreover, nanofibre namely nano-TK01M exhibited the best antifungal activity in inhibiting colony growth and sporangia formation at ED_{50} values of 11 and 3 µg/mL, respectively. Nano-TK01M treated on durian leaves induced the synthesis of scopoletin, which is known as a defense mechanism and marker of plant resistance or plant immunity. Moreover, the application of nano-TK01M significantly reduced disease incidence, the same as metalaxyl. Additionally, nano-TK01M treatment was the most effective in enhancing plant physiological parameters, including the synthesis of chlorophyll, carotenoid contents and promoted plant growth, compared to both metalaxyl and non-treated control. *T. hamatum* K01 produced antifungal metabolite pyrone 6-pentyl-2H-Pyran-2-one and sorbicillin. It is reported for the first time that pyrone and sorbicillin could be expressed as bioactive compounds in reduction of the disease incidence of durian rot caused by *P. palmivora*. The finding confirmed that nano-TK01M from *T. hamatum* K01 exhibited the most effective in controlling plant pathogen, which could be promoted as agricultural input for plant disease management, and it is also a nontoxic fungicide for living life and eco-friendly.

Keywords: Nanofibre, *Trichoderma hamatum*, Phytoalexins, *Phytophthora palmivora*, root rot

How to cite this:

Phal P, Soytong K and Poeaim S. A new nanofibre derived from *Trichoderma hamatum* K01 to control durian rot caused by *Phytophthora palmivora*. Asian J. Agric. Biol. xxxx(x): 2023182. DOI: https://doi.org/10.35495/ajab.2023.182

Introduction

Durian (*Durio zibethinus*) is an essential agricultural commodity in Southeast Asia. This popular fruit has been named the "King of Fruit". Thailand has exported 90% of durian fruit to the global market, which has made Thailand the largest durian exporter globally, followed by Malaysia and Indonesia (Kongtragoul et al., 2021). However, durian cultivation encounters several disease problems, such as stem rot, fruit rot, and root rot pathogens caused by *Pythium* spp., *Phytophthora nicotianae* and *Phytophthora palmivora* (Tongon et al., 2018). *P. palmivora* fungus is the most damaging and economically important pathogen of durian (Vawdrey et al., 2005). This fungus infects all stages of durian, in which the disease symptoms include yellow leaves, twigs dried from the tops, stem rot, and, more importantly, root rot, and the trunk appears to have brown to dark brown sores. The long infection period causes leaves to drop and plants die (Mohamed Azni et al., 2019), causing yield losses and increasing production costs, estimated at 20-25% (Kongtragoul et al., 2021).

Conventionally, synthetic fungicides have been traditionally used for Phytophthora rot management. A total of 21,004 tons of synthetic fungicides were imported to Thailand in 2018, with a price of 687 million U.S. dollars, and have been used to control this pathogen (Kongtragoul et al., 2021). Chemical fungicides are usually applied at least 20 times from production until postharvest. However, it can still reduce the disease level to lower than economic damage. However, long-term use of chemical fungicides induced the pathogen to develop resistance to those chemical fungicides by reducing their effectiveness to the pathogen (Kongtragoul et al., 2021). Phytophthora species have been discovered to resist metalaxyl in various countries, such as Thailand, China, Mexico, the United Kingdom, Morocco, Cameroon, Poland, Russia, Estonia, the United States, and Uganda (Kongtragoul et al., 2021). Due to the pathogen's resistance to chemical compounds, researchers have explored other methods to control this pathogen. Moreover, there is a need for safe foods without chemical contamination and a strong desire to protect the environment (Alabouvette et al., 2006).

Biological control of *Phytophthora* spp. has been reported using *Trichoderma* spp.(Soytong et al., 2013). Christiaan Persoon first identified *Trichoderma* species in 1794. Weindling was the first reporter of its biological control as a mycoparasite against *Scleractinia and Rhizoctonia* in 1934 (Zhang and Zhuang, 2018).

Nanotechnology has been studied for disease management and applied to construct at the atomic level, including the formulation of organic materials as nanoparticles (Tongon and Soytong, 2022). Researchers have recently examined organic nanomaterials for their biological properties (Pan et al., 2019). Active metabolites from natural products are constructed to be nanoparticles that can easily penetrate through plant cells quickly, and they increase the effectiveness of bioactive compounds and decrease leaching from the plant surface after application (Perlatti et al., 2013). Scientists have constructed different types of nanoparticles for disease management (Biswas et al., 2023). Nanofibres from *Chaetomium* spp. expressed antifungal activity actively against plant pathogens (Song et al., 2020). The other study reported by Tongon et al. (2018) found that nanoparticles derived from *Ch. brasiliense* significantly inhibited the growth of *P. palmivora*, is known a causal agent of durian root rot pathogen. Phytoalexins are known as the defence mechanism of plants against pathogenic organisms (Ahuja et al., 2012). Plants are found to produce phytoalexins after being stimulated by chemical and mechanical injury and plant pathogens infection (Singh and Chandrawat, 2017). The accumulation of phytoalexins is induced in plants after applying nanoparticles, which play a role in defense and reduce disease incidences caused by pathogens. Rice leaves treated with nanoparticles from *Ch. brasilience* were found to produce phytoalexins, namely Oryzalexin B and Sakuranertin, as part of their defence mechanisms against *M. oryzae* (Song et al., 2020).

Therefore, our research finding was conducted to isolate *P. palmivora* from the root rot of durian and investigated antifungal activities of *T. hamatum* K01 against *P. palmivora* in vitro. A greenhouse trial was also conducted to examine the effects of nano-TK01M on reduction of severity disease of durian rot caused by *P. palmivora*, plant physiological, plant growth parameters, and determined synthesis of phytoalexins in durian, compared to metalaxyl and non-treated control.

Material and Methods

Source of fungal pathogen and isolation

A soil sample collected from infected durian plant var Monthong showed yellow leaves, twigs died back, and

root rot in Chanthaburi Province, Thailand. The pathogen was isolated using baiting technique. The soil samples 10-20 cm in depth, were collected 3-4 points at the areas where the roots were infected by pathogen and air-dried overnight, then ground and weighed to approximately 20 g and added into sterilized Petri dishes that contained 20 mL of sterilized distilled water. The durian leaves were used as bait, which were collected from healthy durian plants. They were cut into small pieces (3x3mm) in diameter for four pieces, floated in petri dishes, and then incubated for 24-72 hrs at room temperature (27-30 °C). Pieces of bait were left dry for 1 min by sterilized tissue paper before being placed on water agar (WA) plate and incubated for 24-72 hrs at room temperature. Hyphal tips growing in WA were then cut and moved to BNPRA + PDA media, which contained mycostatin (0.5 mg), ampicillin (500 mg), benomyl (20 mg), PCNB (25 mg), and rifampicin (5 mg), and then mixed with 100 mL sterilized water at 45 °C. BNRPA media (40 mL) was mixed into 360 mL of PDA media, potato 2000 g, dextrose 200 g and agar 150 g with 10 L of water. Finally, the colony growth in (BNPRA + PDA) media was cut and transferred to PDA media plates to get the pure culture.

Source of antagonistic fungus

T. hamatum K01 was used as an antagonist, which was offered by Prof. Dr. Kasem Soytong, Department of Plant Production Technology, School of Agricultural Technology, King Mongkut's Institute of Technology Ladkrabang (KMITL), 10520 Bangkok, Thailand.

Identification

Morphological identification of *P. palmivora*

P. palmivora was identified based on morphological characteristics to confirm the species level. It was separately cultured in PDA and V8 juice agar media (V8A; V8 juice 175 mL/L, [Campbell Soup Co., Camden, NJ, USA], 2.5 g/L, CaCO3, 17 g/L, agar 700 mL of water) for seven days at room temperature (27-30 °C). General characteristics and other structures of *P. palmivora* were studied. The sample was mounted on a glass slide, covered with a coverslip, and examined with scanning electron microscopy (SEM) and a light compound microscope.

Morphological identification of the antagonistic fungus

To confirm the species level, *T. hamatum* K01 was morphologically characterized. This fungus was separately grown in PDA medium and V8A at room temperature (27-30 °C) for five days. *T. hamatum* K01 was morphologically identified according to Younesi et al. (2021).

Molecular analysis

Molecular analysis was also performed to identify species of *P. palmivora* and *T. hamatum*. The fungi grew in PDB at room temperature (27-30 °C) for seven days. The mycelia were harvested from PDB through filter paper and ground with liquid nitrogen in a mortar and pestle. Deoxyribonucleic acid (DNA) was extracted using the cetyltrimethyl ammonium bromide (CTAB) method, modified by the protocol of Zhou et al. (2022). A ground powder of biomass (1-2 g) was used for cell extraction. The phenolic compound was separated in the tube by adding 2X CTAB buffer for 700 µL and β-mercaptoethanol for 2 µL and heated for 60 min in a water bath at 65 °C. Chloroform: isoamyl alcohol (24/1) v/v was added to the tube and then centrifuged at 14000 rpm for 5 min. The upper aqueous layer was transferred after centrifugation and treated with RNase for 30 min at 37 °C. Then, 50 µL of 10% CTAB in 0.7 M NaCl was added to the solution, precipitated with cold isopropanol, and rinsed with absolute ethanol and 70% ethanol. The DNA pellet was dried in an incubator at 37 °C before being mixed in T.E. buffer and kept at -20 °C for PCR templates. PCR was operated to amplify the DNA templates. The PCR program modified the method of Grunwald et al. (2011) initial denaturation at 95 °C for 5 min, followed by 94 °C for 1 min, for 35 cycles and 60 °C for 2 min, and at 72 °C for final extension. A master mix of 25 µL for the PCR program was prepared, which contained DNA 1 µL, water NA 14.3 µL, Tag DNA 0.2 µL, Tag Buffer 2.5 µL, dNTP 4 µL, and the universal primer ITS. One microlitre of each primer was used for PCR amplification. ITS1 (5'-TCCGTAGGT-GAACCTGCGG-3') and ITS4 (5'-TCCTCCGCT-TATTGATATGC-3') were applied for the identification of *Trichoderma hamatum*, and ITS4 (5'-TCCTCCGCTTATTG-ATATGC-3') and ITS5 (5'-GAAGGTGAAGTCGTAACAAGG-3') were applied for the identification of *Phytophthora palmivora*. PCR products (5 µL) were electrophoresed in a 1% agarose gel (2 g), and T.E. buffer (50 µL) was added to evaluate the DNA band. DNA sequences were retrieved from GenBank by aligning the sequence from a National Center for Biotechnology Information (NCBI) database using Basic Local Alignment Search Tools (BLAST) analysis. The phylogenetic trees were created using the MEGA-X software.

Pathogenicity test

P. palmivora PYSC01 was proven to be a casual pathogenic organism using the detached leaf method of durian (Var Montong). The experiment was performed using a completely randomized design (CRD) with four replications. *P. palmivora* PYSC01 was separately grown in PDA media for seven days at room temperature (27-30 °C). Leaf samples were obtained from healthy durian plants, the surface was disinfected with 75% ethyl alcohol, and 5-6 perforation wounds were made on the leaves using a sterilized needle. Periphery growth of pathogen 0.5 cm^2 was cut using a sterilized cork borer and then placed onto the wounded leaves, and agar plugs from PDA media were transferred onto the wounded leaves to serve as a control. The detached leaves were kept separately with moist tissue paper in a chamber box for seven days at room temperature (27-30 °C). Data were collected by measuring the brown rot lesions (cm^2) around the pathogen's agar plug using ImageJ software. The percentage of damage was computed using Equation (1)

$$(\%)\ \text{Damage} = \frac{\text{Areas of damage}}{\text{Areas of test leave}} * 100 \quad (1)$$

Isolation of bio compounds from *T. hamatum* K01

Bio compounds were isolated using gas chromatography/mass spectrometer analysis (GC/MS). Bio compounds were elucidated from crude methanol extract by gas chromatography in conjunction with mass spectrometry (GC/MS). In detail, the compounds were analyzed by an Agillen 6890 N gas chromatograph with an Agilent 5973 mass detector equipped with an HP-5 silica capillary column (30 m 0.25 mm ID, 0.25 µL film thickness). The oven temperature program began at 50 °C for 3 min and increased from 10 °C/min to 200 °C for 3 min. Then, the final temperature was increased from 15 °C/min to 260 °C for 20 min. Helium was used as the carrier gas at a flow rate of 1 mL/min. MS analysis was conducted over a detection range of 30–500 amu. The sample was arranged from crude extract: methanol (1/2) g/mL, and sample 0.2 µL was injected with a split ratio of 50:1. The detector and injector temperatures were maintained at 250 °C and 270 °C, respectively. MS analyzed the specific compounds, and their identity was determined by comparing the Kovats retention index with that a homologous series of n-alkanes. Percentage components based on the area of GC peak and time of retention were computed using the data processor Shimadzu CR6A.

Evaluation of *T. hamatum* to control pathogen in *vitro*

Metabolite crude extract test

The antagonistic substances were extracted following Kanokmedhakul et al. (2006). *T. hamatum* K01 was cultivated in potato dextrose broth (PDB) and incubated at room temperature (27-30 °C) for 35 days. Fungal biomass was harvested and air-dried for seven days. Dry biomass was grounded to obtain ground biomass. The antagonistic substance was extracted using hexane, ethyl acetate, and methanol as solvents. Ground biomass was soaked with hexane (1:1 v/v) and shaken for three days, filtrated using filter paper (Watman No 4), and evaporated to obtain crude hexane (TK01-Hexane). The marc was soaked again with ethyl acetate, evaporated to yield crude ethyl acetate (TK01-EtOAc), and finally soaked with methanol and evaporated to yield crude methanol (TK01-MeOH). These crude extracts were tested to inhibit *P. palmivora* PYSC01 using a poisonous food method. The experiment replicated four replications in a 3x6 two-factor factorial design in CRD. Factor (X) was the crude extracts, and factor (Y) was the concentrations of 1000, 500, 100, 50, 10 µg/mL, and 0 µg/mL was served as control. Each crude extract was dissolved in one drop of 2% dimethyl sulfoxide (DMSO), added to molten PDA medium, and autoclaved at 121 °C (15 psi) for 35 min. *P. palmivora* PYSC01 was subcultured in PDA for seven days at room temperature (27-30 °C). Peripheral of *P. palmivora* PYSC01 growing in PDA were cut (0.5 cm^2) using sterilized cork borer and transferred in the middle of (5.0 cm) diameter PDA plates that contained each concentration and incubated until the control plates (0 µg/mL) grew full plates.

Microbial nanofibres test

Nanofibres derived from *T. hamatum* K01 were tested to inhibit *P. palmivora* PYSC01, causing durian rot. The nanofibres were constructed following the method of Dar and Soytong (2014). Each crude hexane, ethyl acetate, and methanol were separately incorporated into polylactic acid (PLA)-based nanofibres through electrospinning to produce nanofibres. Each nanofibre was coded as nano-TK01H, nano-TK01E, and nano-TK01M respectively. The size of each nanofibre was measured and characterized using scanning electron microscopy (SEM). The experiment was replicated four times in a two-factors factorial in CRD. Factor (X) represented by nanofibres, while factor (Y) represented concentrations 15, 10, 3, 5 µg/mL, and 0 µg/mL served as control. Each nanofibre was

dissolved in one drop of 2% dimethyl sulfoxide and mixed with PDA media before autoclaved at 121 °C (15 psi) for 35 min. The culture of the pathogen was cut (0.5 cm^2) at the peripheral mycelia growth using a sterilized cork borer and placed onto the center of (5.0 cm) diameter PDA media petri dishes with each concentration and incubated until the control plates (0 µg/mL) grew fully. The sporangia from each treatment were examined for abnormal sporangia using a light compound microscope.

Data collection and statistical analysis

Data were collected by measuring colony diameter (cm) and number of sporangia formation using a hemocytometer. Data were statistically analyzed using ANOVA. Treatment means were compared with Duncan's multiple range test (DMRT) at $p<0.05$. The effective dose (ED_{50}) was calculated using SPSS Statistics version 28.0.0.0 (190). The percentage for inhibition was computed using Equations (2) and (3)

$$\% \text{ Colony suppression } = \frac{X - Y}{X} * 100 \quad (2)$$

$$\% \text{ Sporangia suppression} = \frac{X1 - Y1}{X1} * 100 \quad (3)$$

Were, X-colony growth in control, Y-colony growth in each concentration, X_1-sporangia formation in control, and Y_1-sporangia formation in each treatment.

Greenhouse experiments

The experiment was done to examine the effect of nano-TK01M from *T. hamatum* K01 and metalaxyl compared to non-treated control on phytoalexin production, disease reduction of durian rot caused by *P. palmivora* PYSC01, plant physiological and plant growth parameters. One year old durian trees var. Monthong were planted in plastic pots (25x16 cm) in diameter with a mixture of loam soil, fine coconut shield, and sand (2:1:1). The durian plants were inoculated with *P. palmivora* PYSC01 at $1x10^6$ spore/mL, and 24 hrs after fungal inoculation, treatments were spayed by nano-TK01M from *T. hamatum* K01 at a rate of 15 µg/mL, metalaxyl at the rate of 1g/L every seven days. The non-treated control was sprayed with water. The experiment was carried out using a randomized completely block design (RCBD) with four replications. Data were statistically analyzed using ANOVA. Treatment means were compared with DMRT at $p<0.05$.

Phytoalexin synthesis

Phytoalexins production in durian was examined through thin layer chromatography (TLC). The samples of durian leaves were collected on days 3, 5, 7, and 14 after treatment. The extraction method was done following Tongon and Soytong (2022) each fresh leaf sample 1 g from each treatment was washed with methanol, then cut into small pieces and ground with a pestle. Next, they were soaked in 10 mL methanol, heated for 90 min in the water bath at 50 °C, then filtrated using filter paper (No. 4, Whatman, UK), and evaporated to yield crude extracts. Each crude extract was dissolved by sterilized water before being spotted on a TLC plate, and standard scopoletin (Sigma Co., Ltd.) was also spotted for comparison. The TLC plate was soaked in developing solvent in a tank that contained 20 mL of acetic acid. The developed chromatograms were dried until spots appeared and examined under UV illumination. The absorbance was measured at 366 nm, and the retention factor (R_f) was computed using Equation (4).

$$Rf = \frac{\text{Distance traveled by the compound}}{\text{Distance traveled by a mobile phase}} \quad (4)$$

Disease reduction

Disease reduction (DR) was examined on days 30 and 60 after fungal inoculation and nano-TK01M and metalaxyl treatment. Fifteen leaves of durian counted from the top were selected and disease symptoms were observed, such as yellow leaves, died back from the tip, and leaves dropped in control and treatment. The percentage of infection was computed using Equation (5), described by Mergawy et al. (2023).

$$\% \text{ DI} = \frac{\text{Number of infected leaves}}{\text{Total number of tested leaves}} * 100 \quad (5)$$

Disease level was classified into five levels, modified the method of El-Sharkawy et al. (2023) where 0=no symptom, 1=1-25%, 2=26-50%, 3=51-75%, and 4=76-100%. Disease severity (DS) was computed using Equation (6), and disease reduction was calculated using Equation (7) Masoud et al. (2023).

$$\% \text{ DS} = \frac{\text{Total number of infected leaves} * \text{level of disease}}{\text{The number of tests leaves} * \text{the highest disease level}} * 100 \quad (6)$$

$$\% \text{ DR} = \frac{\text{DS in control} - \text{DS in treatment}}{\text{DS in control}} * 100 \quad (7)$$

Physiological parameters

Chlorophyll and carotenoid contents were examined after nano-TK01M and metalaxyl treatment on day 60. A sample of durian leaves 0.1 g was weighted using an electronic balance, then extracted with 5 mL of 80% acetone using mortar and pestle, then centrifuged at 10000 rpm for 20 min, and the final volume of 10 mL was adjusted by adding 80% acetone. Absorbance was read at 663nm, 647nm, and 470nm for chlorophyll (a, b) and carotenoids, respectively, and pigment amount was computed using Lichtenthal's Equation following the method of Emamverdian et al. (2021).

$C_a\,(\mu g/g) = 12.25A_{663} - 2.79A_{647}$

$C_b\,(\mu g/g) = 21.50A_{647} - 5.10A_{663}$

$C_{x+c}\,(\mu g/g) = (100A_{470} - 1.82C_a - 85.02C_b)/198$

Where C_a=chlorophyll a, C_b=chlorophyll b, C_{x+c}= carotenoid, and A= wavelength of sunlight absorbance

Assessment of growth parameter

The experiment evaluated the efficacy of nano-TK01M from *T. hamatum* K01 and metalaxyl on the growth parameter of durian regarding plant height under greenhouse conditions. The assessment was done before and on days 30 and 60 after treatment.

Results

Isolation and morphological identification

Morphological identification of *P. palmivora* PYSC01 and *T. hamatum* K01

The results showed that isolated PYSC01 had grown fully in 9 cm diameter PDA petri dish at day eight. The colony's characteristics presented stellate mycelium that was cotton white, uniformly grown, and slightly diffuse. Under a light compound microscope, hyphae were nonseptate, hyaline, undulating, and lumpy, branching of 3.5-4.9 µm in width. Sporangia were produced by inflation from the tips of the branch of the sporangiophore and exhibited different shapes: elongate ellipsoid, lemon-shaped, and ovoid. Sporangia were 24.7-41 µm in diameter with a mean of 28.5 µm and 11.4-30 µm in length with a mean of 18.3 µm, and the papilla was a conic protuberance or small and rounded with a size of 2.8-4.2 µm; the papilla was generally translucent, pore at papillae of the sporangia released the zoospores. Oogonium is a smooth wall 24.2x34.5 µm diameter and spherical, short, and cylindrical with a single antheridium. Sporangiophores are thin, proliferation, and globose or subglobose chlamydospores ranging from 15.1-34.5 µm in length and 15.6-24.6 µm in width (Fig 1.). *T. hamatum* K01 from the previous study of Phal et al. (2023) was also confirmed by its morphological characteristics. The identification results showed that the colony appearance is thin white to brown on the surface, and when it is older, the color changed to yellow on the reverse side, it is pure yellow on the upside down. Scanning electron microscopy (SME) indicated that the culture was whip-like, smooth-walled, with hyphal elongations of 2.8 to 5.7 µm. The culture showed roughened conidiophores with a size of 3.2 to 18.3 µm with granules, and these conidiophores produced phialides conidia 2.7 to 4.1 µm in width, 3.8 to 5.7 µm in length and germination of chlamydospores.

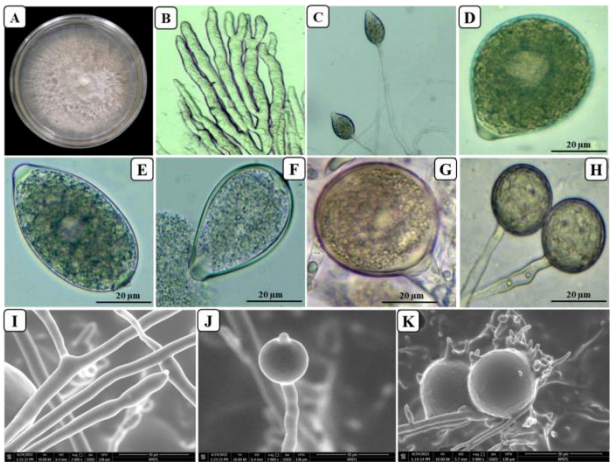

Figure-1. Morphologically characterized *P. palmivora* PYSC01. a colony appearance in PDA at ten days old. b, i, lumpy-branding mycelia. d, e, sporangia with different shapes. f zoosporangia released from sporangia. g one antheridium with one oogonium. c, j, occurrence of sporangia on sympodium and h, b, chlamydospore. b-h were observed under a light compound microscope, and i-k were observed using scanning electron microscopy (SEM).

Molecular analysis of *P. palmivora* PYSC01 and *T. hamatum* K01

The results indicated that the isolate PYSC01 ITS5-4 was the same clade as HQ237479 *Phytophthora palmivora*, MH219857 *Phytophthora palmivora*, LC684558 *Phytophthora palmivora*, MH219852 *Phytophthora palmivora*, LC684540 *Phytophthora palmivora*, GU111683 *Phytophthora arecae* and KP050545 *Phytophthora taxon banihhashemiana*. EF025942 *Colletotrichum gloeosporioides* were compared as an outgroup. *Trichoderma hamatum* K01-ITS1 is the same clade with *Trichoderma*

hamatum AB737864 isolate FKI-6011, *Trichoderma hamatum* MW750434 isolate GL19, *Trichoderma hamatum* OL439486 strain Th23, *Trichoderma hamatum* MW763159 isolate TISC-3, *Trichoderma hamatum* MN880214 strain JAHLH2, and *Trichoderma hamatum* KX424842 isolate NGL1, with *Colletotrichum gloeosporioides* EF025942 Cm 89 compared as an outgroup (Fig 2.).

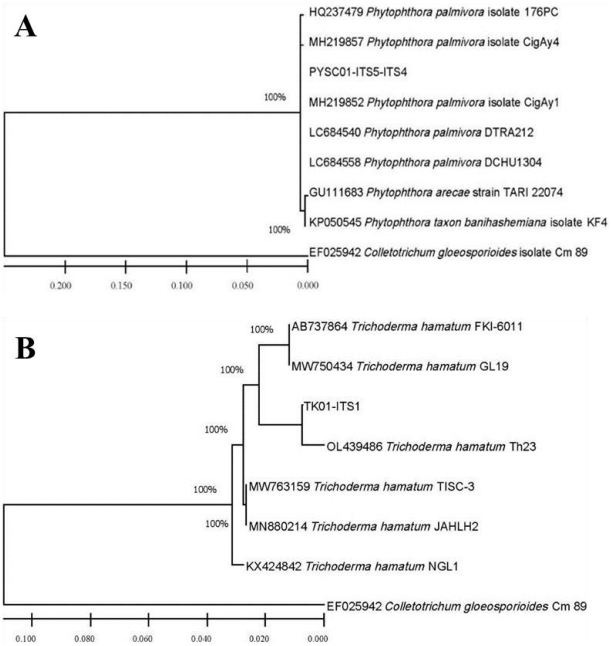

Figure-2. Phylogenetic trees were constructed with 100% bootstrap value using the distance-based analysis of the universal primers ITS and the 5.8S region of the rDNA. The tree was searched in GenBank to determine the phylogenetic relationship. a *P. palmivora* PYSC01, b *T. hamatum* K01.

Table-1. Measurement of damaged durian leaves using ImageJ software.

Reps.	Areas of test leaves (cm^2)	Areas of damaged (cm^2)	% damaged
1	45.18	12.68	28.07%
2	58.40	5.84	10.00%
3	50.55	6.66	13.17%
4	48.78	6.78	13.90%
Percentage of damaged of four replications			16.29%

Pathogenicity test

The results indicated that the inoculation of *P. palmivora* PYSC01 infected durian leaves within three days. The detached leaves presented water-soaked dark brown around the agar plugs of the pathogen. On day 5, the lesions were measured with a 2.5-3 cm diameter disease lesion and computed 16.29 % using ImageJ software, as shown in Table 1. The lesion expanded more extensively with the long inoculation period. While the non-inoculated controls did not show any disease symptoms, they remained healthy.

Biocompound from *T. hamatum* K01

GC/MS analysis indicated that *T. hamatum* K01 produced 34 constituents that detected 97.37% of the total crude methanol. The most abundant compounds are pyrone, namely 6-pentyl-2H-Pyran-2-one, with 16.61 min, and Miscellaneous (Sorbicillin), with a 20.90 min retention time, based on the total area of the GC/MS analysis. These compounds have been reported to possess antifungal property.

Evaluation of *T. hamatum* K01 against *P. palmivora* isolate PYSC01

Crude extracts test

The results indicated that three crude extracts exhibited a broad spectrum of action against *P. palmivora* isolate PYSC01 at 10-1000 µg/mL concentrations. Among these crude extracts, crude TK01-MeOH was the most effective on colony growth and sporangia formation inhibition, in which ED_{50} values were computed by 288 and 118 µg/mL, respectively. Followed by crude TK01-EtOAc, in which the sporangia inhibition was computed at ED_{50} value of 185 µg/mL. While the lesser effect was recorded with crude TK01-hexane, the ED50 in colony growth and sporangia inhibition required higher than 1000 µg/mL. However, sporangia formation was more sensitive than colony growth to all crude extract tests (Table 2.). Moreover, *T. hamatum* K01 was found to produce lysis enzymes, as evidenced by the crude extract test casing abnormal sporangia formation.

Table-2. Crude extracts from *T. hamatum* K01 against *P. palmivora*

Crude extracts	Concentrations (µg/mL)	Colony growth (cm)	Growth inhibition (%)	ED_{50} (µg/mL)	Sporangia production (10^4)	Inhibition (%)	ED_{50} (µg/mL)
Hexane	0	4.95^{a}	-	-	81.75^{a}	-	-
	10	4.90^{a}	1.01^{ef}		79.50^{a}	2.75^{ef}	
	50	4.72^{ab}	4.65^{ef}		68.50^{b}	16.21^{de}	
	100	4.30^{bc}	13.13^{d}		66.60^{b}	18.53^{d}	
	500	3.32^{d}	32.93^{c}		61.75^{b}	24.46^{d}	
	1000	3.05^{d}	38.38^{c}		43.25^{c}	47.09^{c}	

EtOAc	0	4.95[a]	-	-	81.75[a]	-	185.00
	10	4.50[a]	9.09[de]		79.00[a]	3.36[ef]	
	50	4.10[d]	17.17[d]		62.00[b]	24.16[d]	
	100	3.27[ef]	33.94[c]		42.00[c]	48.62[c]	
	500	2.97[ef]	40.00[c]		26.00[d]	68.20[b]	
	1000	2.35[g]	52.53[b]		19.25[de]	76.45[ab]	
MeOH	0	4.95[a]	-	288.66	81.75[a]	-	118.92
	10	4.12[d]	16.77[d]		72.50[ab]	11.31[def]	
	50	3.15[ef]	36.36[c]		49.75[c]	39.14[d]	
	100	2.92[f]	41.01[c]		40.00[c]	51.07[c]	
	500	2.40[g]	51.52[b]		25.00[de]	69.42[ab]	
	1000	1.90[h]	61.62[a]		15.00[e]	81.65[a]	
C.V. (%)	-	6.28	21.65		12.58	28.21	
The average of four replications, the means followed by the same letters are not significantly different between treatments based on Duncan's multiple range test (DMRT) at $p<0.05$							

Table-3. Testing nanofibres from *T. hamatum* K01 against *P. palmivora*

Nanofibres	Concentrations (µg/mL)	Colony growth (cm)	Growth inhibition (%)	ED_{50} (µg/mL)	Number of spores (10^5)	Inhibition (%)	ED_{50} (µg/mL)
TK01H	0	4.77[a]	-	19.96	27.00[a]	-	9.83
	3	3.70[b]	22.43[f]		26.00[ab]	3.70[e]	
	5	3.52[b]	26.21[f]		22.50[ab]	16.67[e]	
	10	3.02[c]	36.69[de]		10.00[cd]	62.96[bc]	
	15	2.67[cde]	44.03[bcd]		5.50[de]	79.63[ab]	
TK01E	0	4.77[a]	-	16.66	27.00[a]	-	5.48
	3	3.62[b]	24.11[f]		20.50[b]	24.07[d]	
	5	3.40[bc]	28.72[ef]		13.75[c]	49.07[cd]	
	10	3.02[cd]	36.69[de]		3.75[e]	86.11[ab]	
	15	2.40[e]	49.69[bc]		0.25[e]	99.07[a]	
TK01M	0	4.77[a]	-	11.06	27.00[a]	-	3.13
	3	2.85[cd]	40.25[cd]		14.50[c]	46.30[cd]	
	5	2.47[de]	48.22[bc]		4.75[de]	82.41[ab]	
	10	2.35[e]	50.73[b]		1.50[e]	94.44[a]	
	15	1.80[f]	62.26[a]		0.00[e]	100.00[a]	
CV%	-	7.89	17.72		29.28	32.87	
The average of four replications, the means followed by the same letters are not significantly different between treatments based on Duncan's multiple range test (DMRT) at $p<0.05$							

Natural product nanofibres test

Nanofibres (nano-TK01H, nano-TK01E, and nano-TK01M) were characterized, and the size (diameter) was measured using SME ranging between 75-168, 57-242, and 90-256 nm, respectively. They were tested to suppress *P. palmivora* PYSC01 at 3-15 µg/mL concentrations. The results indicated that nano-TK01M exhibited highly significant colony growth and sporangia inhibition at ED_{50} values of 11.06 and 3.13 µg/mL, respectively. Moreover, sporangia were not produced at a 15 µg/mL concentration. However, nano-TK01E inhibited colony growth and sporangia formation at ED_{50} values of 16.66 and 5.48 µg/mL, respectively. There was a lesser effect on colony growth and sporangia from nano-TK01H, for which the ED_{50} values were computed at 19.96 and 9.83 µg/mL, respectively (Fig. 3 and Table 3.).

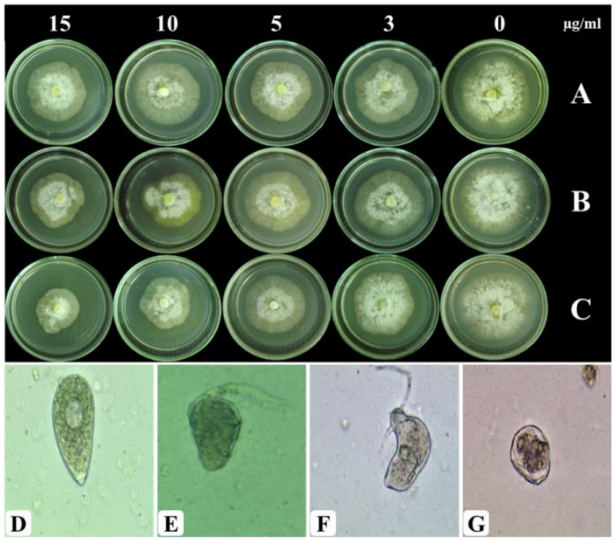

Figure-3. Microbial nanofibres derived from *T. hamatum* K01 against *P. Palmivora* PYSC01. a, b, and c tested nano-TK01H, nano-TK01E and nano-TK01M on the growth of *P. palmivora* PYSC01, respectively. d normal sporangia formation of *P. palmivora*. e, f, and g abnormal sporangia formation of *P. palmivora* caused by nano-TK01H, nano-TK01E, and nano-TK01M, respectively.

Greenhouse experiments

Phytoalexin synthesis

Phytoalexin production in durian was examined on days 3, 5, 7, and 14 after treatment. The result indicated that the application of nano-TK01M at 15 µg/mL, along with the inoculation of *P. palmivora* PYSC01, led to the production of phytoalexin as observed by the presence of a clear blue spot compared to standard scopoletin, while the application of metalaxyl and non-treated control showed unclear blue spots on TLC plate on day 14 after treatment (Fig. 4). Under UV light at 365 nm, R_f value was measured to be 0.78, which was determined to be scopoletin.

Disease reduction

Nano-TK01M from *T. hamatum* K01 and metalaxyl were treated to suppress durian rot caused by *P. palmivora* PYSC01. The application of metalaxyl showed the highest significant disease reduction by 83% and 99.60%, followed by nano-TK01M 72.50 and 99.17 % on days 30 and 60, respectively, compared to the non-treated control, as shown in Table 4. In the non-treated control, the durian plants

exhibited symptoms such as yellowing leaves, drying of twigs, dying back starting from the tips, and leaves dropped and plant died, consistent with the symptoms observed in the durian garden. However, the durian plants treated with nano-TK01M and metalaxyl did not exhibit any disease symptoms and remained healthy.

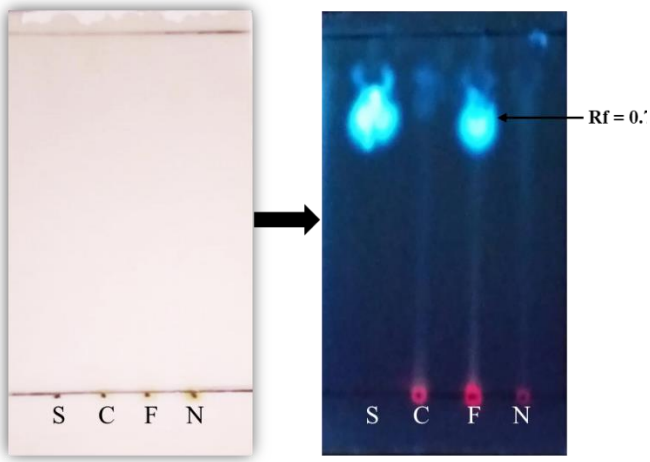

Figure-4. The presence of phytoalexin of scopoletin on a TLC plate at R_f value of 0.87 under UV light of 365 nm, S standard scopoletin, C non-treated control, F nano-TK01M, and N metalaxyl.

Table-4. Effects of nano-TK01M from *T. hamatum* K01 and metalaxyl on reduction of disease incidence of durian.

Treatment	Day 30 after treatment			Day 60 after treatment		
	DI (%)	DS (%)	DR (%)	DI (%)	DS (%)	DR (%)
Control	25.00a	10.00^{a}	-	96.66^{a}	96.66^{a}	-
Nano-TK01M	6.6^{b}	1.6^{b}	72.50^{a}	3.30^{b}	0.83^{b}	99.17^{a}
Metalaxyl	3.3^{b}	0.83^{b}	83.33^{a}	1.70^{b}	0.41^{b}	99.60^{a}
CV %	76.77	103.26	71.00	15.72	11.57	1.73

The average of four replications means in a column followed by a joint letter does not different statically by Duncan's multiple range test (DMRT) at *p<0.05*. DI- disease incidence, DS- disease severity, DR- disease reduction.

Plant physiological parameters

The data of plant physiological parameters regarding chlorophyll and carotenoid contents were examined on day 60 after treatment. The maximum of chlorophyll contents and carotenoid were recorded in the treatment of nano-TK01M, 25.98 and 3.70 µg/g, respectively, followed by treatment of metalaxyl 16.30 and 2.15 µg/g, as compared to the non-treated control 10.07, and 1.65 µg/g, respectively (Table 5.).

Table-5. Effects of nano-TK01 derived from *Trichoderma hamatum* K01 and metalaxyl on chlorophyll contents of durian plants.

Treatments	Chlorophyll (Chl) contents (µg/g)			
	Chl_a	Chl_b	Total Chl	Carotenoid
Control	7.49^{b}	2.57^{b}	10.07^{b}	1.65^{a}
Nano-TK01M	18.84^{a}	7.14^{a}	25.98^{a}	3.70^{a}
Metalaxyl	12.13^{ab}	4.16^{ab}	16.30^{ab}	2.15^{a}
CV%	27.56	31.43	28.13	30.14

Means followed by the same letter are not significantly different at p<0.05.

Plant growth parameter

The application of nano-TK01M and metalaxyl significantly increased plant height parameter over control. Nano-TK01M was the most effective treatment, in which plant height parameter was increased by 74.25 and 76.25 cm, followed by metalaxyl 69.50 and 72.50 cm. The lowest effect was recorded in non-treated control 69 and 64.78 cm on days 30 and 60 after treatment, respectively, as shown in Table 6.

Table-6. Effects of nano-TK01M derived from *T. hamatum* K01 and metalaxyl on height of durian plants.

Treatments	Plant height parameter (cm)		
	Before treatment	After treatment	
		Day 30	Day 60
Control	69.00^{a}	67.25^{b}	64.87^{b}
Nano-TK01M	69.25^{a}	74.25^{a}	76.25^{a}
Metalaxyl	67.00^{a}	69.50^{ab}	72.50^{a}
CV%	3.25	3.92	3.68

Means followed by the same letter are not significantly different at p<0.05.

Discussion

Phytophthora root rot is the most severe disease on durian plantations in Thailand and other Southeast Asian countries. *P. palmivora* PYSC01 was obtained from the root zone of durian infected by root rot disease. The fungus was proven to be an aggressive pathogen causing durian rot using Koch's postulate, similar to the study of Mohamed Azni et al. (2019). The external characteristics showed that *P.*

palmivora PYSC01 produced a different shape of sporangia with one papilla, branched hyphae, and globose chlamydospores, as confirmed by the report of Suksiri et al. (2018). *T. hamatum* K01 was morphologically identified. The colony pattern and cultural characterization corresponded to the study of Mao et al. (2020). Moreover, the results of molecular characterization indicated that the isolate PYSC01 common ancestors GenBank accession numbers HQ237479, MH219857, LC688458, MH219852, and LC684540, with EF025942 as the outgroup, similar to the one reported by Tongon and Soytong (2021). For molecular phylogeny of antagonist, *Trichoderma hamatum* K01 is closely related to the sequences of *Trichoderma hamatum* of the GenBank accession numbers MW750434, AB737864, MN880214, OL439486, KX424842, and MW763159, which was recorded with a 100% bootstrap value, and built after the distance-based analysis of the universal primers ITS1, ITS4, and 5.8S rDNA sequences, confirmed by the report of Abdelkhalek et al. (2022).

Trichoderma species have been reported to produce cell wall-degrading enzymes (β-1,3 glucanases, β-1,4 glucanases, proteases, and chitinases) (Baazeem et al., 2021). These defense enzymes can decay the cell wall of oomycetes pathogens (Dourou and La Porta, 2023). Our research indicated that crude extract from *T. hamatum* K01 exhibited an antibiotic substance to suppress both colony growth and sporangia formation of *P. palmivora* PYSC01. The difference in crude extract produces a variety of bioactive compounds with various fungal activities and molecular weights, resulting in variations in efficacy (Yassin et al., 2021), which can be illustrated by the difference in crude extract in the variation response against *P. palmivora* PYSC01. It was indicated that bioactive substances involving crude TK01-MeOH exhibited the strongest antifungal activity to inhibit colony growth and sporangia formation, with ED_{50} values of 288.66 and 118.92 µg/mL, respectively. Moreover, crude TK01-EtOAc gave a better effect for inhibition than crude TK01-Hexane and was the least effective on both colony growth and sporangia formation. A previous report by Kaewchai and Soytong (2010) found that the metabolite crude methanol from *T. hamatum* STN07 exerted the best potential activities in the host plant directly by the production of the bioactive compound to suppress the *Rigidoporus microporus,* causing rubber white root disease, in which colony growth was inhibited by 80% at a 500 µg/mL concentration with an ED_{50} value of 187 µg/mL, while crude hexane extract was the least effective. Similarly, the biological control agent *T. hamatum* THSW13 was reported to suppress the growth of *P. capsici*, causing damping-off collar rot pathogens of chili pepper seedlings by 61% (Chemeltorit et al., 2017).

The study highlighted that nanofibres derived from *T. hamatum* K01 could be used at low concentrations to inhibit *P. palmivora* PYSC01. Nano-TK01M suppressed colony growth and sporangia formation of *P. palmivora* PYSC01 at ED_{50} values of 11 and 3 µg/mL, respectively. Nano-TK01E gave ED_{50} values of 16 and 5 µg/mL, respectively, and Nano-TK01H ED_{50} values were computed at 19 and 9 µg/mL, respectively. El-Wakil (2020) found that silver nanoparticles from *T. hamatum* significantly inhibited colony soil-borne pathogens (*Fusarium* spp., *F. semitectum, F. solani, F. roseum,* and *F. oxysporum).* Similarly, species of Chaetomium are also reported to utilize their bio substances to control *P. palmivora* and are known to be causal agents of durian rot. For instance, nanofibres (nano CC-H, nano CC-E, and nano CC-M) from *Ch. cupreum* reported promising and varying inhibition against *P. palmivora*, inhibiting colony growth at ED_{50} values of 1.78, 1.51, and 1.19 µg/mL, respectively, and reducing sporangia production at ED_{50} values of 13.03, 11.01 and 16.48 µg/mL, respectively (Tongon and Soytong, 2022). This study showed that the inhibitory effects in crude extracts and nanofibre tests are related to major pyrone metabolites (6-pentyl-2H-pyran-2-one), and sorbicillin was produced from *T. hamatum* K01, which acted as an antifungal metabolite against *P. palmivora* PYSC01. This study was supported by Reino et al. (2008), who found that pyrone metabolite (6-pentyl-2H-pyran-2-one) was produced from *Trichoderma harzianum*, *Trichoderma viride*, and *Trichoderma koningii*. This metabolite inhibited colony growth of *R. salani* 69.6% and completely suppressed spore production of Fusarium at 0.45 mg/mL. Several other studies indicated that antifungal metabolites such as pyrone (6-pentyl-2H-pyran-2-one) and sorbicillin are commonly produced by Trichoderma species. These metabolites have been found to suppress the growth of pathogenic organisms significantly (Ngo et al., 2021; Phal et al., 2023).

Another main finding is that durian plant inoculated with *P. palmivora* PYSC01 and treated with antimicrobial nano-TK01M from *T. hamatum* K01 led to induce the production of phytoalexin namely

scopoletin with R_f values of 0.78, which is considered as the marker of plant disease resistance or plant immunity. The research finding is consistent with the finding of Tongon and Soytong (2022), who detected synthesis of phytoalexin in durian leaves treated with nanoparticles loaded by crude ethyl acetate from *Chaetomium cupreum* and inoculated with *P. palmivora* found to produce scopoletin with the R_f values of 0.75, in which this scopoletin role as a defense mechanism against *P. palmivora*, is known a causal agent of durian rot. Scopoletin synthesis was also found in tobacco. This compound expressed antimicrobial potential toward *Alternaria alternata*, causing tobacco disease (Sun et al., 2014). Additionally, applying nano-TK01M from *T. hamatum* K01 under greenhouse conditions significantly reduced disease severity and incidence of durian rot caused by *P. palmivora* PYSC1, the same as the application of metalaxyl. This research finding was confirmed by Mau et al. (2022) in a greenhouse experiment indicated that *T. hamatum* treatment was the most effective in decreasing brown spot pathogens caused by *D. oryzae* by 36.42 %, compared to fungicide Trivia 73 WP 28.62%. Similarly, Alfaro-Vargas et al. (2022) revealed that peptaibol from *Trichoderma asperellum* treatment completely reduced disease incidence by 100 % of tomatoes caused by *Alternaria alternata* the same as a chemical fungicide (clotrimazole) compared to untreated control. A similar result was reported by Hammad et al. (2021), who discovered that *T. brevicompactum* (isolate TBS1) significantly decreased the grey mould incidence of tomatoes caused by *Botrytis cinerea* by 64.43%. The disease incidence of charcoal rot of lentil plant caused by *Macrophomina pseudophaseolina* was reduced by 91.7% at day 40 after application of *T. longibrachiatum*, compared to non-treated control (Kouadri et al., 2023). This inhibitory effect is due to the stimulation of systemic resistance (Mergawy et al., 2023) and antifungal metabolite synthesis (Garnica-Vergara et al., 2016). In addition, nano-TK01M from *T. hamatum* K01 treatment showed the most effective synthesis of chlorophyll (a, b) and carotenoid contents and increased plant height parameters higher than metalaxyl as compared to non-treated control. These parameters are enhanced by the interaction between nano-TK01M with the plants due to the decreasing durian rot incidence caused by *P. palmivora* and increased photosynthesis of chlorophyll and carotenoid contents, which helped improve root function and nutrient adsorption. A similar result reported by Choudhary and Ashraf (2019) who found that *Trichoderma harzianum* treatment gave the best enhancement of photosynthesis of chlorophyll and carotenoid contents and increased plant growth parameters of mungbean. The application of Trichoderma species resulted in the enhancement of chlorophyll photosynthesis through the synthesis of chloroplast enzymes (Shoaib et al., 2018), promoted plant growth through the improvement of micronutrient adsorption and availability of nutrients to plants, reduced the disease incidence through the production of secondary metabolites in various plants (Ketta and Hewedy, 2021)

Conclusion

P. palmivora PYSC01 was identified based on its morphology and ITS rDNA sequence and confirmed as a causal pathogen of durian rot. Nano-TK01M from *T. hamatum* K01 exhibited the best growth inhibition of *P. palmivora* PYSC01 and reduced disease incidence of durian rot caused by *P. palmivora*, the same as metalaxyl. This study suggests that the antagonistic fungus *T. hamatum* K01 plays an essential role in controlling *P. palmivora*, is known as a causal agent of durian rot. This can be a promising option for plant disease protection in the fields in the future while ensuring sustainable production that is friendly for farmers, consumers, and the environment. This research finding is limited to the efficacy of nanofibres from *T. hamatum* K01 against Phytophthora rot of durian in vitro and pots experiment. Further research may consider investigation in the field experiment and evaluate its inhibitory effect against other plant pathogens in vitro and field trials.

Acknowledgment

We would like to acknowledge the KMITL Doctoral Scholarship 2019, King Mongkut's Institute of Technology Ladkrabang (KMITL), Ladkrabang, Bangkok 10520, Thailand, offers the research project to be successfully done.

Disclaimer: None.
Conflict of Interest: None.
Source of Funding: This work was funded by King Mongkut's Institute of Technology Ladkrabang, (KMITL), Thailand under Grant KDS2019/027.

Contribution of Authors

Phal P: Contributed in conceptualization, methodology, formal analysis, investigation, writing original draft, visualization, literature review and editing of the manuscript.
Soytong K: Contributed in conceptualization, methodology, editing of manuscript and supervision.
Poeaim S: Editing of manuscript and supervision.

References

Abdelkhalek A, Al-Askar AA, Arishi AA and Behiry SI, 2022. *Trichoderma hamatum* strain th23 promotes tomato growth and induces systemic resistance against tobacco mosaic virus. J. Fungi, 8(3): 228. Available from https://doi.org/10.3390/jof8030228.

Ahuja I, Kissen R and Bones AM, 2012. Phytoalexins in defense against pathogens. Trends Plant Sci., 17(2): 73-90. Available from https://doi.org/10.1016/j.tplants.2011.11.002.

Alabouvette C, Olivain C and Steinberg C, 2006. Biological control of plant diseases: The european situation. Plants, 114(3): 329-341. Available from https://doi.org/10.1007/s10658-005-0233-0.

Alfaro-Vargas P, Bastos-Salas A, Muñoz-Arrieta R, Pereira-Reyes R, Redondo-Solano M, Fernández J, Mora-Villalobos A and López-Gómez JPJJoF, 2022. Peptaibol production and characterization from trichoderma asperellum and their action as biofungicide. J. Fungi, 8(10): 1037. Available from https://doi.org/10.3390/jof8101037.

Baazeem A, Almanea A, Manikandan P, Alorabi M, Vijayaraghavan P and Abdel-Hadi A, 2021. In vitro antibacterial, antifungal, nematocidal and growth promoting activities of *trichoderma hamatum* fb10 and its secondary metabolites. J. Fungi, 7(5): 331. Available from https://doi.org/10.3390/jof7050331.

Biswas P, Polash SA, Dey D, Kaium MA, Mahmud AR, Yasmin F, Baral SK, Islam MA, Rahaman TI and Abdullah A, 2023. Advanced implications of nanotechnology in disease control and environmental perspectives. Biomed. Pharmacother., 158: 114172. Available from https://doi.org/10.1016/j.biopha.2022.114172.

Chemeltorit PP, Mutaqin KH and Widodo W, 2017. Combining *trichoderma hamatum* thsw13 and pseudomonas aeruginosa bj10–86: A synergistic chili pepper seed treatment for *phytophthora capsici* infested soil. Eur. J. Plant Pathol., 147(1): 157-166. Available from https://doi.org/10.1007/s10658-016-0988-57984375

Choudhary A and Ashraf S, 2019. Utilizing the combined antifungal potential of trichoderma spp. And organic amendments against dry root rot of mungbean. J. Biol. Pest Control, 29(1): 83. Available from https://doi.org/10.1186/s41938-019-0187-8.

Dar J and Soytong K, 2014. Construction and characterization of copolymer nanomaterials loaded with bioactive compounds from chaetomium species. Int. J. Agric. Technol., 10(4): 823-831.

Dourou M and La Porta CAMJJoF, 2023. A pipeline to investigate fungal–fungal interactions: Trichoderma isolates against plant-associated fungi. J. Fungi, 9(4): 461. Available from https://doi.org/10.3390/jof9040461.

El-Sharkawy HHA, Abo-El-Wafa TSA, Mostafa NA and Yousef SAM, 2023. Boosting biopesticide potential of *trichoderma harzianum* for controlling the downy mildew and improving the growth and the productivity of king ruby seedless grape. J. Biol. Pest Control, 33(1): 61. Available from https://doi.org/10.1186/s41938-023-00707-x.

El-Wakil DA, 2020. Antifungal activity of silver nanoparticles by trichoderma species: Synthesis, characterization and biological evaluation. Egypt J Phytopatho, 48(1): 71-80. Available from https://doi.org/10.21608/ejp.2020.49395.1015.

Emamverdian A, Ding Y, Barker J, Mokhberdoran F, Ramakrishnan M, Liu G and Li Y, 2021. Nitric oxide ameliorates plant metal toxicity by increasing antioxidant capacity and reducing pb and cd translocation. Antioxidants, 10(12): 1981. Available from https://doi.org/10.3390/antiox10121981.

Garnica-Vergara A, Barrera-Ortiz S, Muñoz-Parra E, Raya-González J, Méndez-Bravo A, Macías-Rodríguez L, Ruiz-Herrera LF and López-Bucio J, 2016. The volatile 6-pentyl-2h-pyran-2-one from *trichoderma atroviride* regulates arabidopsis thaliana root morphogenesis via auxin signaling and ethylene insensitive 2 functioning. New Phytol., 209(4): 1496-1512. Available from https://doi.org/10.1111/nph.13725.

Grunwald N, Martin F, Larsen M, Sullivan C, Press C, Coffey M, Hansen E and Parke J, 2011.

Phytophthora-id.Org: A sequence-based phytophthora identification tool. Plant Dis., 95(3): 337-342. Available from https://doi.org/10.1094/PDIS-08-10-0609.

Hammad M, Guillemette T, Alem M, Bastide F and Louanchi M, 2021. First report of three species of trichoderma isolated from the rhizosphere in algeria and the high antagonistic effect of *trichoderma brevicompactum* to control grey mould disease of tomato. J. Biol. Pest Control, 31(1): 85. Available from https://doi.org/10.1186/s41938-021-00423-4.

Kaewchai S and Soytong K, 2010. Application of biofungicides against rigidoporus microporus causing white root disease of rubber trees. Int. J. Agric. Technol., 6(2): 349-363.

Kanokmedhakul S, Kanokmedhakul K, Nasomjai P, Louangsysouphanh S, Soytong K, Isobe M, Kongsaeree P, Prabpai S and Suksamrarn A, 2006. Antifungal azaphilones from the fungus *chaetomium cupreum* cc3003. J. Nat. Prod., 69(6): 891-895. Available from https://doi.org/10.1021/np060051v.

Ketta HA and Hewedy OAE-R, 2021. Biological control of phaseolus vulgaris and pisum sativum root rot disease using trichoderma species. J. Biol. Pest Control, 31(1): 96. Available from https://doi.org/10.1186/s41938-021-00441-2.

Kongtragoul P, Ishikawa K and Ishii H, 2021. Metalaxyl resistance of *phytophthora palmivora* causing durian diseases in thailand. Hortic., 7(10): 375. Available from https://doi.org/10.3390/horticulturae7100375.

Kouadri MEA, Bekkar AA and Zaim S, 2023. First report of using *trichoderma longibrachiatum* as a biocontrol agent against *macrophomina pseudophaseolina* causing charcoal rot disease of lentil in algeria. J. Biol. Pest Control, 33(1): 38. Available from https://doi.org/10.1186/s41938-023-00683-2.

Mao T, Chen X, Ding H, Chen X and Jiang X, 2020. Pepper growth promotion and fusarium wilt biocontrol by *trichoderma hamatum* mht1134. Biocontrol Sci Technol., 30(11): 1228-1243. Available from https://doi.org/10.1080/09583157.2020.1803212.

Masoud HM, Megahed AA, Helmy MSE, Ibrahim MA-A, El-Mougy NS and Abdel-Kader MM, 2023. Phytopathological and biochemical impacts of *trichoderma harzianum* and certain plant resistance inducers on faba bean root rot disease. J. Biol. Pest Control, 33(1): 63. Available from https://doi.org/10.1186/s41938-023-00709-9.

Mau YS, Prayetno RS, Kaka H, Naat KD, Henuk JBD, Hahuly MV, Widinugraheni S and Gandut YRY, 2022. Efficacy of indigenous trichoderma isolates of west timor, indonesia, as biocontrol agents of brown spot (*drechslera oryzae*) on two upland rice varieties. J. Biol. Pest Control, 32(1): 62. Available from https://doi.org/10.1186/s41938-022-00559-x.

Mergawy MM, Hassanin MMH, Ali AAM and Yousef H, 2023. Morphological characterization, fungicidal alternatives and biological control of peronospora farinosa on chamomile. J. Biol. Pest Control, 33(1): 68. Available from https://doi.org/10.1186/s41938-023-00713-z.

Mohamed Azni INA, Sundram S and Ramachandran V, 2019. Pathogenicity of malaysian *phytophthora palmivora* on cocoa, durian, rubber and oil palm determines the threat of bud rot disease. For. Pathol., 49(6): e12557. Available from https://doi.org/10.1111/efp.12557.

Ngo MT, Van Nguyen M, Han JW, Park MS, Kim H and Choi GJ, 2021. In vitro and in vivo antifungal activity of sorbicillinoids produced by *trichoderma longibrachiatum*. J. Fungi, 7(6): 428. Available from https://doi.org/10.3390/jof7060428.

Pan C, Zhai J and Wang ZL, 2019. Piezotronics and piezo-phototronics of third generation semiconductor nanowires. Chem. Rev., 119(15): 9303-9359. Available from https://doi.org/10.1021/acs.chemrev.8b00599.

Perlatti B, de Souza Bergo PL, Fernandes JB and Forim MR, 2013. Polymeric nanoparticle-based insecticides: A controlled release purpose for agrochemicals. In: Insecticides-development of safer and more effective technologies. IntechOpen: pp: 524-550.

Phal P, Soytong K and Poeaim S, 2023. Natural product nanofibers derived from *trichoderma hamatum* k01 to control citrus anthracnose caused by *colletotrichum gloeosporioides*. Open Agric., 8(1): 1-15. Available from https://doi.org/10.1515/opag-2022-0193.

Reino JL, Guerrero RF, Hernández-Galán R and Collado IG, 2008. Secondary metabolites from species of the biocontrol agent trichoderma. Phytochem. Rev., 7(1): 89-123. Available from https://doi.org/10.1007/s11101-006-9032-2.

Shoaib A, Munir M, Javaid A, Awan ZA and Rafiq M, 2018. Anti-mycotic potential of trichoderma spp. And leaf biomass of azadirachta indica against the charcoal rot pathogen, macrophomina phaseolina (tassi) goid in cowpea. J. Biol. Pest Control, 28(1): 26. Available from https://doi.org/10.1186/s41938-018-0031-6.

Singh R and Chandrawat KS, 2017. Role of phytoalexins in plant disease resistance. Int J Curr Microbiol App Sci, 6: 125-129. Available from http://dx.doi.org/10.20546/ijcmas.2017.601.016.

Song J, Soytong K, Kanokmedhakul S, Kanokmedhakul K and Poeaim S, 2020. Antifungal activity of microbial nanoparticles derived from chaetomium spp. Against *magnaporthe oryzae* causing rice blast. Plant Prot. Sci., 56(3): 180-190. Available from https://doi.org/10.17221/41/2019-PPS.

Soytong K, Chamaiporn C and Somdej K, 2013. Evaluation of microbial elicitors to induce plant immunity for tomato wilt. Afr. J. Microbiol. Res., 7(19): 1993-2000. Available from https://doi.org/10.5897/AJMR12.120.

Suksiri S, Laipasu P, Soytong K and Poeaim S, 2018. Isolation and identification of phytophthora sp. And pythium sp. From durian orchard in chumphon province, thailand. Int. J. Agric. Technol., 14: 389-402.

Sun H, Wang L, Zhang B, Ma J, Hettenhausen C, Cao G, Sun G, Wu J and Wu J, 2014. Scopoletin is a phytoalexin against *alternaria alternata* in wild tobacco dependent on jasmonate signalling. J. Exp. Bot., 65(15): 4305-4315. Available from https://doi.org/10.1093/jxb/eru203.

Tongon R and Soytong K, 2021. Application of *chaetomium cochliodes* cth02 to against durian root rot cause by *phytophthora palmivora* rt01. Int. J. Agric. Technol., 17(2): 753-766.

Tongon R and Soytong K, 2022. Nanoparticles derived from active metabolites of *chaetomium cupreum* cc3003 against phytophthora rot of durian. Int J Agric Biol., 27(1): 19-27. Available from https://doi.org/10.17957/IJAB/15.1894.

Tongon R, Soytong K, Kanokmedhakul S and Kanokmedhakul K, 2018. Nano-particles from *chaetomium brasiliense* to control phytophthora palmivora caused root rot disease in durian var montong. Int. J. Agric. Technol., 14(7): 2163-2170.

Vawdrey LL, Martin TM and De Faveri J, 2005. A detached leaf bioassay to screen durian cultivars for susceptibility to *phytophthora palmivora*. Australas. Plant Pathol., 34(2): 251-253. Available from https://doi.org/10.1071/AP05005.

Yassin MT, Mostafa AA-F and Al-Askar AA, 2021. In vitro antagonistic activity of trichoderma harzianum and t. Viride strains compared to carbendazim fungicide against the fungal phytopathogens of sorghum bicolor (l.) moench. J. Biol. Pest Control, 31(1): 118. Available from https://doi.org/10.1186/s41938-021-00463-w.

Younesi H, Bazgir E, Darvishnia M and Chehri K, 2021. Selection and control efficiency of trichoderma isolates against *fusarium oxysporum* f. Sp. Ciceris in iran. Physiol Mol Plant Pathol., 116: 101731. Available from https://doi.org/10.1016/j.pmpp.2021.101731.

Zhang Y-B and Zhuang W-Y, 2018. New species of trichoderma in the harzianum, longibrachiatum and viride clades. Phytotaxa, 379(2): 131-142. Available from https://doi.org/10.11646/phytotaxa.379.2.1.

Zhou W, Soghigian J and Xiang Q-Y, 2022. A new pipeline for removing paralogs in target enrichment data. Syst. Biol., 71(2): 410-425. Available from https://doi.org/10.1093/sysbio/syab044.